Journal of Metals, Materials and Minerals, 34(1), 1898, 2024

Effect of two-stage heat treatment on the microstructure and mechanical properties of high chrome austenitic manganese steel

Mohammad Reza HERMAWAN[1,2,*], Budi Hartono SETIAMARGA[2], Ilham Nur HAKIM[2], and Rizka Mulia ANGGRAENI[2]

[1] *Department of Mechanical Engineering, Faculty of Engineering, Universitas Pasundan, Bandung 40153, Indonesia*
[2] *Department of Materials Science and Engineering, Faculty of Mechanical and Aerospace Engineering, Bandung Institute of Technology, Bandung 40116, Indonesia*

***Corresponding author e-mail**: rezahermawan@unpas.ac.id

Received date:
23 November 2023
Revised date
4 January 2024
Accepted date:
13 February 2024

Keywords:
Austenitic manganese steel;
Dispersed hardened austenite;
Two-stage heating

Abstract

In this research, heat-treatment was used to determine changes in the microstructure and mechanical characteristics of austenitic manganese steel equivalent to ASTM A128-C. Carbide formed in as-cast conditions is transformed into dispersed hardened austenite to increase the toughness of the material because it can inhibit dislocation movement. Heat treatment is carried out in two heating stages. The first stage of heating was carried out at a temperature of 625°C with a holding time varying by 2.5, 3.5, and 4.5 h, and the second stage was carried out at a temperature of 1000°C with a constant holding time of 1.5 h. Microstructure observations were carried out to observe the structural morphology and carbide transformation in both the first and second stages of heating. Tensile and hardness tests were also carried out to determine the mechanical properties and their effect on two-stage heating. The research results show that the pearlite structure is formed in the first stage of heating with different lamella thicknesses. With the help of ImageJ software, the measured pearlite fraction was higher as the holding time increased in the first stage of heating. This affects the morphology of the carbide colonies formed in the second stage of heating. The higher the pearlite fraction, the more uniform the morphology of the carbide formed with round shapes that are more evenly distributed. These dispersed carbide colonies can increase the toughness of the material up to 17 times higher than the as-cast condition obtained through mechanical testing.

1. Introduction

Austenitic manganese steel is extensively utilized in industrial and heavy equipment requiring strong abrasion and impact resistance [1-3]. This use is made possible by the unique mechanical qualities of austenitic manganese steel, which include excellent toughness, ductility, hardness, and abrasion resistance [1,4]. Due to the formation of carbide precipitates, austenitic manganese steel in its as-cast state is very brittle and lacks the necessary physical characteristics to survive impact. It is possible to increase the mechanical characteristics of austenitic manganese steel with the addition of alloying elements [5,6], heat treatment [7,8], and work hardening [9,10,11]. Solution treatment is one of the heat treatments that may be used to enhance the mechanical characteristics of austenitic manganese steel. As-cast structures must be solution-treated at austenitic temperature for a particular amount of time and then water-quenched in order to get a complete austenite structure [7,12,13]. The austenite phase increases because of the high manganese concentration will act an austenite stabilizer [7,14]. The austenitizing temperature and holding time have a considerable impact on the final phase. When a solution-treated austenitic manganese steel undergoes plastic deformation, the FCC lattice, which has a greater slip system and generates extremely big dislocation movements, gains strength [11]. This process is characterized by an increase in surface hardness after plastic deformation of austenitic manganese steel by either impact or abrasion loads [5,10,15].

Early works have reported the formation of dispersed hardened austenite occurs via a heat treatment procedure, which involves subjecting the casting to a temperature of 595°C and maintaining it at that level for a duration of 8 h to 12 h [16]. This results in the formation of significant quantities of pearlite within the structure. Subsequently, the material is subjected to a temperature of 980°C in order to enhance the structural integrity. This process transforms regions of pearlite into a finely grained austenite that contains a distribution of tiny carbide particles. These particles are unable to dissolve as long as the temperature of the austenization process does not surpass 1010°C. In addition, the fast-cooling procedure will result in the formation of dispersion-hardened ausnetite. This type of ausnetite is known for its increased yield strength; higher hardness; and reduced ductility compared to the steel that undergoes complete or full solution treatment at elevated austenitization temperatures. The dispersion-hardening heat treatment permits the incorporation of a comparatively elevated carbon content, hence enhancing the resistance to abrasion.

Modification of the microstructure by forming spherical carbides is also carried out on medium-carbon steel to increase toughness and flexibility through heat treatment [17], with the formation mechanism shown in Figure 1. Spheroidization was carried out at a constant temperature of 700°C with a spheroidization time of 8 h, 12 h and 16 h. In this study, it was found that spheroidizing time had the greatest influence on the percent spheroidized, and the initial microstructure contributed 31.1%.

This research will focus on increasing the toughness and surface hardness of austenitic manganese steel equivalent to ASTM A128 Grade C. This material was chosen because it has a higher chromium content compared to other grades. The formation of dispersed carbide colonies is the aim of this research, which is expected to increase the toughness of the material because these carbide colonies can hinder dislocation movement. So, a high chromium content, such as in grade C, can help research because chromium is a carbide formation. The process of forming carbide colonies, which we call dispersed hardened austenite, is carried out through two-stage heating. In the first stage of heating, the carbide from metal casting is transformed into pearlite, and then the pearlite is transformed into small carbide colonies with an austenite matrix in the second stage of heating. However, this research is also limited to observing morphology through microstructure and tensile and hardness tests to determine the effect of carbide colonies on mechanical properties, especially toughness and hardness, without observing in more detail the type and properties of the carbide.

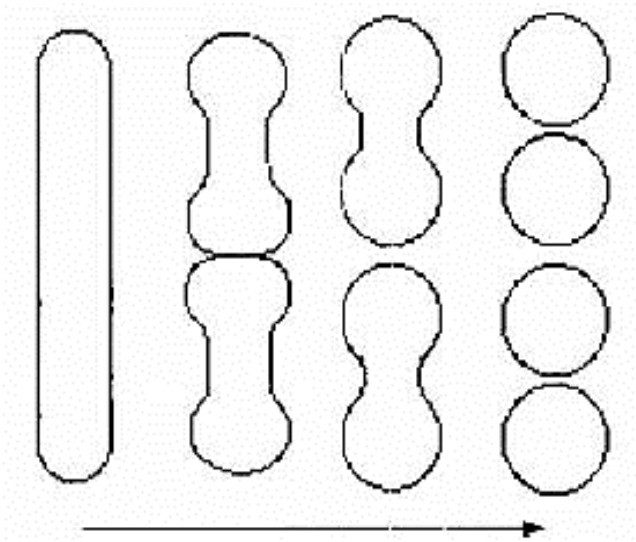

Figure 1. Mechanism of formation dispersed hardened austenite [17].

2. Experimental

2.1 Materials

As stated in Table 1, the material employed in this investigation is austenitic manganese steel with a high chromium concentration which is equivalent to ASTM A128 grade C. Since chromium is a carbide formation, the chromium alloy element in this research has more chromium to facilitate the production of dispersed hardened austenite during the heat treatment procedure [5,18,19]. In this investigation, samples were taken from metal casting operations that used a high-frequency crucible induction furnace powertrack 150 R to 30 R and a pouring temperature of 1500°C in the foundry laboratory of the Bandung Manufacturing Polytechnic. High-manganese steel scrap that has been melted with other metal alloys serves as the raw material. To reduce casting product flaws, a Y-block mold is being employed.

2.2 Method

Y-block samples obtained from metal casting results were then cut and fabricated into samples for tensile testing, hardness testing, metallographic testing, scanning electron microscopy (SEM), and x-ray diffraction (XRD). Optical Electron Spectrometry (OES) was utilized to analyze chemical composition using a Thermo Scientific machine of the ARL3460 model. At room temperature, ASTM E8-compliant tensile test samples were prepared on a Zwick-Roell Z250 machine with a constant loading rate of 1 $mm \cdot min^{-1}$. A micro vickers FR-1e was used to analyze the hardness of a specimen with a minor load of 98.07 N, a major load of 980.7 N, and a holding time of 15 s. The microstructural analysis was performed using the metallographic method; in accordance with ASTM E3-01 specifications; and SEM for high magnification. A D8 advance Bruker machine was used to conduct XRD analysis on samples that had undergone mechanical treatment and those that had only undergone heat-treatment.

The mechanical properties of the material were investigated using as-cast and heat-treated samples. Using the Nabertherm Muffle Furnace L3/11 heat-treatment furnace with Flap Door, the heat-treatment process was conducted in two phases of heating, with the first stage heating at a temperature of 625°C and the second stage heating at a temperature of 1000°C. The variations of heat treatment process shown in Table 2. Experiments were conducted to determine the optimal structural morphology and mechanical properties generated by a two-stage solution treatment by altering the heating duration in the first stage at 625°C.

Table 1. Chemical composition of the research samples.

Material	C (%)	Mn (%)	Cr (%)	Si (%)	P (%)
Austenitic manganese steels	1.21	12.8	2.5	0.76	0.006

Table 2. Variations in heat treatments processes.

Sample	Temperature in stage 1 (°C)	Holding time in stage 1 (h)	Temperature in stage 2 (°C)	Holding time in stage 2 (h)
1	625	2.5	1000	1.5
2	625	3.5	1000	1.5
3	625	4.5	1000	1.5

3. Results and discussion

3.1 Microstructure analysis

For as-cast and as-treated samples with three types of metallographic examinations have been conducted. As illustrated in Figure 2, the microstructure of the as-cast sample comprises of carbide and austenite as the major phases. This austenite phase is the result of a high manganese concentration, an austenite stabilizer [7,20]. At the grain boundaries, this material's carbides exhibit both lamellar and acicular structures. According to the phase equilibrium diagram for Fe-Mn, this material is hyper-eutectoid, hence cementite forms at the grain boundaries. Due to this feature, this material has the propensity to create austenite-based pre-eutectoid cementite. Carbides generated near grain boundaries are often an issue, since their presence may induce cracking, rendering the material incapable of withstanding strong mechanical stresses.

With a solution treatment technique [21,22], the carbide at this grain boundary may be converted into a pearlite phase. The creation of pearlite is initiated by the nucleation of Fe_3C cementite in austenite grains [23,24]. Cementite develops by the diffusion of carbon atoms, hence, a layer of ferrite forms surrounding cementite in areas of carbon deficit [25].

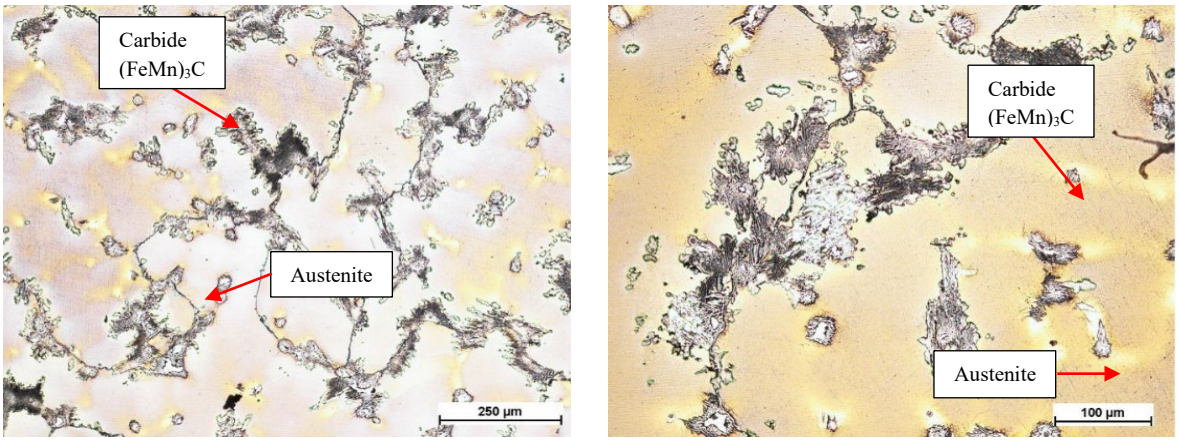

Figure 2. Microstructure of as cast condition.

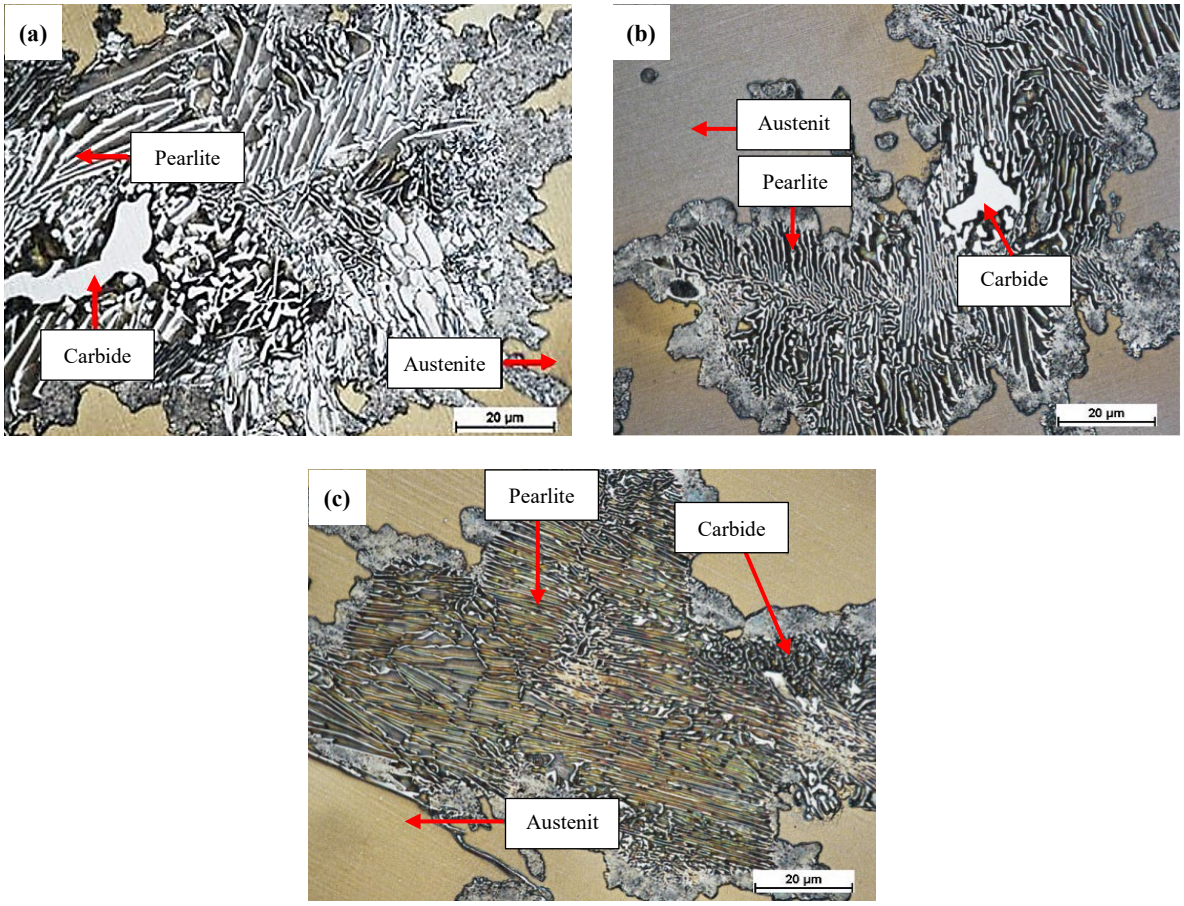

Figure 3. The microstructure formed in the first stage of heating, (a) at a holding time of 2.5 h, (b) at a holding time of 3.5 h, and (c) at a holding time of 4.5 h.

During the first phase of heating, carbide grain boundaries was converted into pearlite. At this point in the heating process, temperature and time influence the diffusion of carbon atoms. The lower temperature slows the diffusion of carbon atoms, resulting in a shorter diffusion distance and a thinner lamella, while the holding time influences the quantity of carbon atoms that may diffuse. As illustrated in Figure 3, carbon atoms disperse more the longer the holding time.

A quantitative study was performed using the ImageJ program [26], to confirm that more pearlite structures were created as the holding time increased in the first heating step, with the findings displayed in Figure 4. Based on these findings, it is obvious that the holding time has an effect on the carbon atoms that may disperse, hence influencing the pearlite structure that forms.

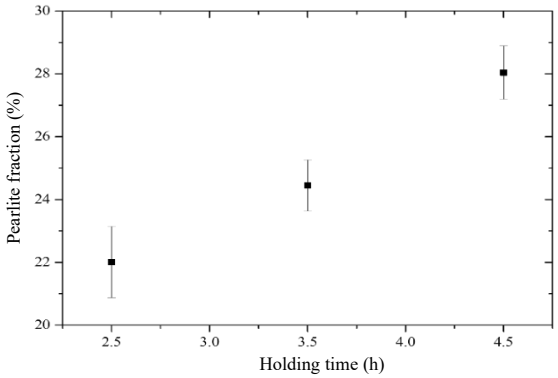

Figure 4. Pearlite fraction curve.

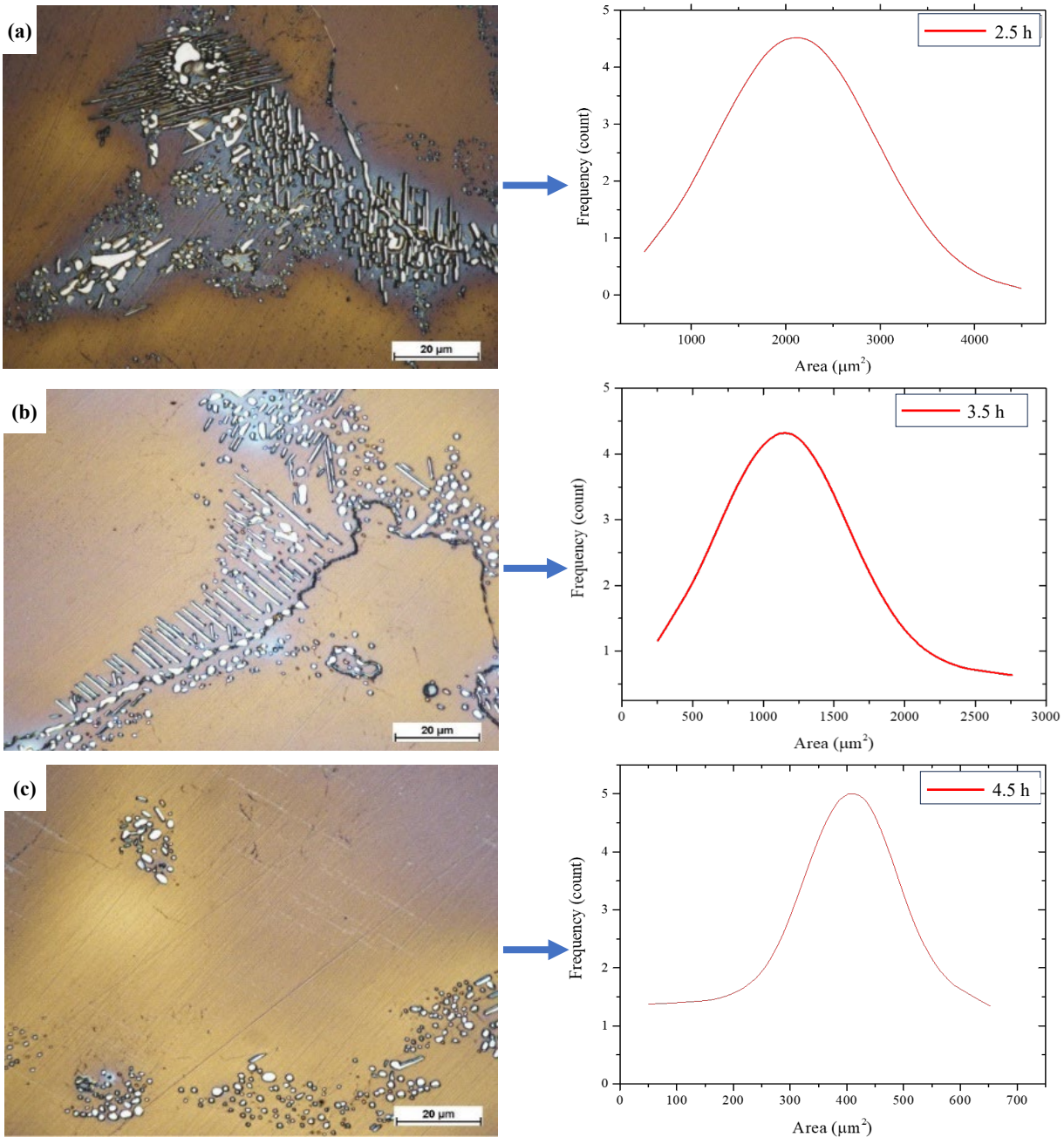

Figure 1. Carbide morphology develops during two-stage heating and area of carbide colonies at (a) 2.5 h, (b) 3.5 h, and (c) 4.5 h of holding time in the first stage of heating.

The heating temperature was set at 1000°C in the second stage of heating with a holding time of 1.5 h for all samples; both samples were heated for 2.5 h, 3.5 h, and 4.5 h in the first stage of heating, then quenched with agitated water media. Pearlite, which was created during the first step of heating, is converted into carbide colonies known as distributed hardened austenite during this stage of heating. The metallographic findings in Figure 5 show that a two-stage heating procedure was used to effectively generate dispersed hardened austenite. The carbide was purposefully not totally dissolved during the creation of this microstructure because this carbide is believed to be able to survive the movement of dislocations without losing the ductile qualities of austenitic manganese steel.

Figure 5 shows variations in the shape of dispersed hard austenite as well as variations in holding time applied to the preheating cycle and the graph to the right is an estimate of the area of dispersed hardened austenite carbide colonies measured using ImageJ software [26]. On the graph, the Y axis shows the frequency or number of dispersed hardened austenite grains contained in the sample and the X axis shows the size of the dispersed hardened austenite. The curve's shape suggests that the colonies created are of varying sizes, with the area values that occur most often found near the curve's greatest peak. The lowest area was 407 μm^2 as a result of heat treatment with 4.5 h holding time and the greatest area was 2106 μm^2 as a result of a 2.5 h holding time. The findings from these tests show that the longer the holding time in the first heating step, the smaller the carbide area. In this situation, the pearlite morphology created during the first step of heating may be the source of the production of carbide colonies in various places. In two-stage heating, the fineness of the lamellae in pearlite determines the production of dispersed hardened austenite carbide colonies.

SEM characterization was performed where there were carbide colonies with spherical and lamellar morphologies to identify the morphology of disseminated hardened austenite, as illustrated in Figure 6. Based on the driving force in thermodynamics, which comes from the decrease in energy between the carbide surface and the matrix. These different forms of secondary carbides occur due to the inhomogeneous distribution of driving force kinetics, which is a diffusion phenomenon from the carbide surface into the matrix. Qualitatively characterized in Figure 6, where round carbides are represented by dotted lines in rectangular sections and lamellar carbides are represented by continuous lines. Several pearlite structures are produced during the first step of heating. This is due to the various carbide sizes and holding times during the first heating. The observed pearlite microstructure is divided into two types: fine and coarse pearlite. Since the cementite lamellae in fine pearlite are thinner, the lamellae and solvent separation requires less time than in coarse pearlite. As a result, the rate of rounding off carbide colonies in fine pearlite microstructure is faster than in coarse pearlite.

3.2 Mechanical properties analysis

Tensile and hardness tests are used to evaluate mechanical characteristics. The toughness value is computed in the tensile test using the equation Ut=u+y2x f [21] where Ut is tensile toughness, u is ultimate tensile strength, y is yield strength, and f is elongation. Relative toughness is added as a comparison between the results of the thermal treatment procedure and the as-cast material's toughness values with the test results and calculations provided in Table 3.

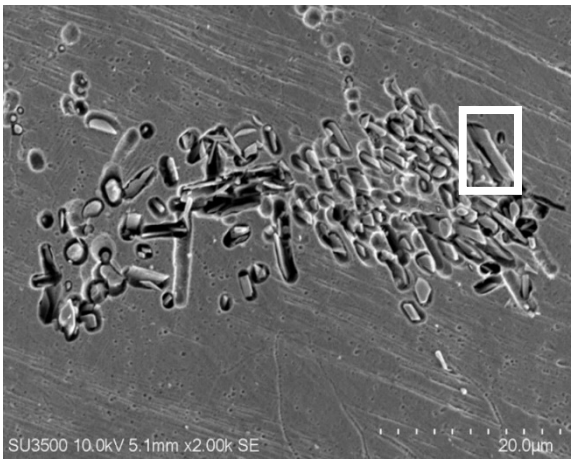

Figure 6. Carbide morphology in other colony areas in spherical and lamellar forms from a holding time of 2.5 h in stage one heating

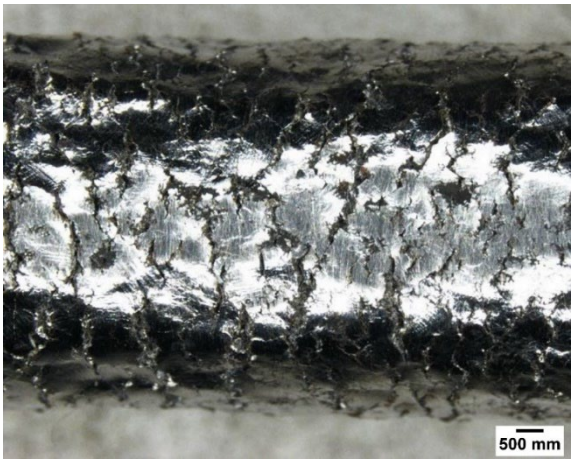

Figure 7. The phenomenon of orange peeling on the gage length surface.

Table 3. Tensile test result.

Sample	Yield Strength (Mpa)	Tensile Strength (Mpa)	Elongation (%)	Toughness ($J \cdot m^{-3}$)	Relativet Toughness
as-cast	366	573	2.6	12.2	1
as-treated 2.5 h holding time	364	814	31.5	182.5	15.2
as-treated 3.5 h holding time	344	811	35.4	204.5	16.7
as-treated 4.5 h holding time	336	806	36.2	206.6	16.9

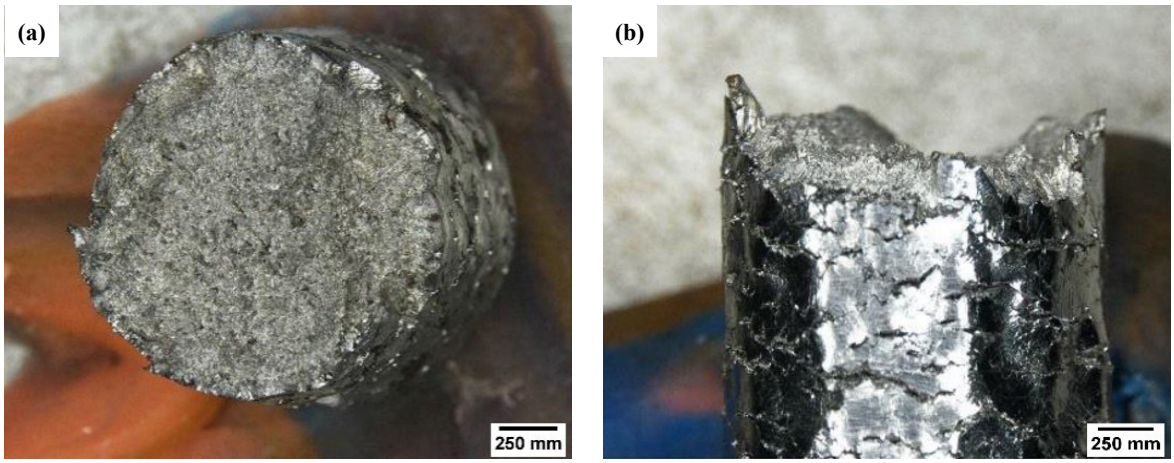

Figure 8. Fracture of the tensile test specimen. (a) top view, (b) side view.

The as-cast sample with a toughness of 12.2 $J \cdot m^{-3}$ has the lowest value due to the presence of carbide at the grain boundaries. This carbide renders the material brittle, resulting in a poor toughness rating. In contrast, the as-heat treated sample had a substantially greater toughness owing to the dissolving of carbide at the grain boundaries, which resulted in the formation of distributed austenite carbide colonies. The relationship between the colony size and distribution of dispersed hardened austenite carbides and the ultimate tensile strength and elongation values is very close. The increased holding time in the first step will reduce the yield strength and ultimate tensile strength, but increase the elongation. Hence, the holding time procedure in stage one effects the tensile strength of this material; the longer the holding time, the higher the tensile strength.

On the gage length surface of the tensile test specimen, as seen in Figure 7, there occurs an intriguing occurrence known as orange peeling. Immediately upon yielding, this process causes crinkling and the creation of fissures on the gage-length surface. Depending on grain orientation; grain size; and the presence of inhibitors in the crack propagation mechanism [27], the fracture that results from an orange peeling event propagates to a particular depth inside the specimen. The presence of dispersed hardened austenite carbide, which is generated by two-stage heating, is crucial for inhibiting fracture development towards the interior of the gage length. The surface fractures are induced not only by grain boundary cracking, but also by martensite developed on the surface as a consequence of plastic deformation during the tensile test, which results in a shearing mechanism. As is well knowledge, martensite is hard and brittle.

The "orange peeling" effect is induced by austenite grains on the gage-length surface that have an active slip system as a result of plastic deformation during the tensile test. A twin deformation strengthening mechanism will emerge from the grain orientation, which features an active slip system on the gage length surface. This result is in accordance with the result of M. Abbasi, *et al.* [27] and Rittel, *et al.* [28].

Twin deformation causes twin planes to develop in an austenite grain, dividing it into n-parts. These two planes are known as "twin boundary". The presence of twin boundaries might impede the mobility of dislocations, resulting in the buildup of dislocations on the twin boundaries conferring high hardness and strength [5,28,29]. Since austenite grains with twin borders are strong, they cannot accept the grains' stretching and crinkling shapes. This material's orange peeling phenomena is created by a mix of cracking and crinkling. Grain boundary cracking and the martensitic transformation process induce cracking, whereas the twin strengthening mechanism causes crinkling. Figure 8 depicts the kind of fracture that occurs in the as-treated specimen. The fracture tends to be flat, indicating that the fracture type is brittle. The mechanism of martensitic transformation and twinning transformation creates no necking phenomena during the hardening process [30], therefore orange peeling and brittle fracture are extremely likely to occur in this material as a result of martensitic and twinning transformation.

Figure 9 depicts the findings of metallography performed on a gage length exposed to a tensile test to check that martensite forms appropriately in this material.

Based on the results of the XRD test on samples that were only subjected to two-stage heating without any mechanical treatment, martensite with the formation of an alpha prime peak was confirmed, as shown in Figure 10. The appearance of martensite peaks in samples that were only subjected to two-stage heating was likely caused by friction during the sample cutting process and plastic deformation during the grinding and polishing process. While the material that has been mechanically treated after two phases of heating exhibits an increase in martensite structure intensity of the martensite structure and formed an alpha prime peak.

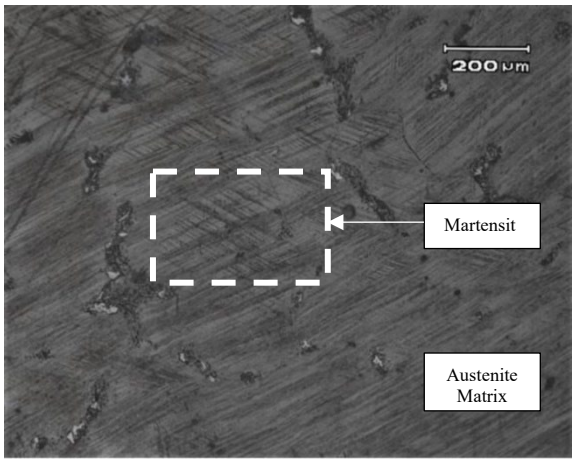

Figure 9. The microstructure of the material after two stages of heating and plastic.

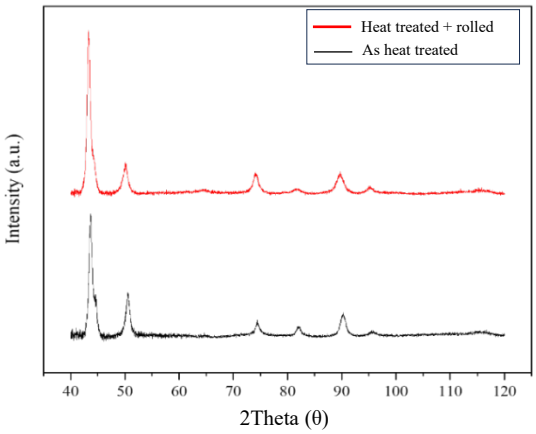

Figure 10. XRD test results on samples that were only subjected to two-stage heating.

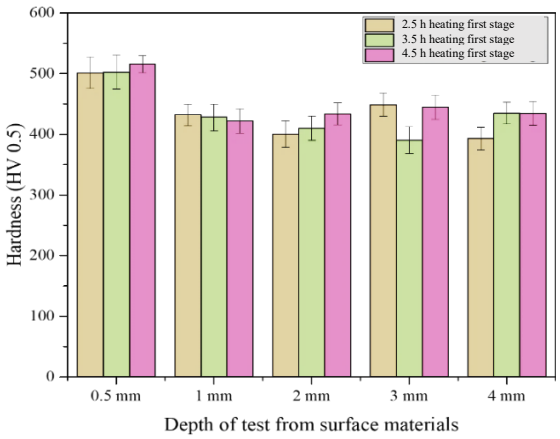

Figure 11. Micro-Vickers hardness value curve on samples that have been subjected to two stages of heating.

In addition to the mechanical characteristics arising from the tensile test, the gage-length cross-section of the plastically deformed tensile test specimen was subjected to Micro-Vickers hardness testing. Up to a depth of 4 mm, the testing procedure is conducted on the surface-proximal portion. As with the tensile test, this hardness test was conducted on all samples that had been heated in two stages, both as heat-treated samples in the variation of the first stage holding time of 2.5 h, as heat-treated samples in the variation of the first stage holding time of 3.5 h, and as heat-treated samples in the variation of the first stage holding time of 4.5 h with the hardness value curve depicted in Figure 11.

The hardest surface has the greatest hardness rating based on the three hardness test findings shown above. Figure 7 illustrates the presence of crinkcling on the surface, which are a result of grain boundary cracking and the martensitic transformation mechanism. This suggests that the surface exhibits greater brittleness, a characteristic that is substantiated by the results of the hardness test. The hardness result was not uniform in the hardness test performed at a depth of 2 mm to 4 mm. This occurs as a result of the indentation process. The indenter may come into contact with grain boundaries, martensite, or dispersed hardened austenite carbide colonies. The indentation process results in a wide, non-uniform dispersion of hardness. Because of the high carbon concentration in these sections, grain boundary and dispersed hardened austenite have high hardness values.

4. Conclusion

Two-stage heating with the first stage at 625°C with holding times of 2.5 h, 3.5 h, and 4.5 h and the second stage at 1000°C and holding time of 1.5 h on high-chromium austenitic manganese steel material creates dispersed hardened austenite, an austenite phase with fine carbide colonies. The heating period of the first stage influences the pearlite fraction, which refines the carbide grains and elongates the space between colonies on distributed hardened austenite carbide when heated in the second stage at 1000°C for 1.5 h. This materials toughness may be increased to 17 times its as-cast value with a two-stage heating procedure. This rise in toughness value is followed by an extension of the initial holding time. The increase in tensile strength is proportional to the duration of the first step of heating. Due to the production of martensitic and twinning transformations at the surface, excessive plastic deformation of this material will result in an increase in surface hardness.

References

[1] S. Kuyucak, "Austenitic manganese steel castings," in *Metallograhy and Microstructures*, ASM International, 2004, pp. 701-718.

[2] N. Tsujimoto, "Casting practice of abrasion resistant austenitic manganese steel," *International Journal of Cast Metals Research*, vol. 4, no. 2, pp. 62-77, 1979.

[3] Z. Pei, R. Song, Q. Ba, and Y. Feng, "Dimensionality wear analysis: Three-body impact abrasive wear behavior of a martensitic steel in comparison with Mn13Cr2," *Wear*, vol. 414, pp. 341-351, 2018.

[4] P. N. Bidulya, and A. Troitsky, *Технология Стальных Отливок. Steel Foundry Practice. Translated... by Anatoly Troitsky*. Peace Publishers, 1965.

[5] C. Chen, F. C. Zhang, F. Wang, H. Liu, and B. D. Yu, "Effect of N^+ Cr alloying on the microstructures and tensile properties of Hadfield steel," *Materials Science and Engineering: A*, vol. 679, pp. 95-103, 2017.

[6] S. Alyaz, "Effects of heat treatment and chemical composition on microstructure and mechanical properties of hadfield steels," Middle East Technical University, 2003.

[7] S. Hosseini, and M. B. Limooei, "Optimization of heat treatment to obtain desired mechanical properties of high carbon Hadfield steels," *World Applied Sciences Journal,* vol. 15, no. 10, pp. 1421-1424, 2011.

[8] M. Azadi, A. M. Pazuki, and M. J. Olya, "The effect of new double solution heat treatment on the high manganese Hadfield steel properties," *Metallography, Microstructure, and Analysis*, vol. 7, pp. 618-626, 2018.

[9] B. Bal, "A study of different microstructural effects on the strain hardening behavior of Hadfield steel," *International Journal of Steel Structures*, vol. 18, pp. 13-23, 2018.

[10] P. H. Adler, G. B. Olson, and W. S. Owen, "Strain hardening of Hadfield manganese steel," *Metallurgical and Materials Transactions A*, vol. 17, pp. 1725-1737, 1986.

[11] H. Bhadeshia and R. Honeycombe, *Steels: microstructure and properties*. Butterworth-Heinemann, 2017.

[12] Y. N. Dastur, and W. C. Leslie, "Mechanism of work hardening in Hadfield manganese steel," *Metallurgical transactions A*, vol. 12, pp. 749-759, 1981.

[13] B. Hutchinson, and N. Ridley, "On dislocation accumulation and work hardening in Hadfield steel," *Scripta Materialia*, vol. 55, no. 4, pp. 299-302, 2006.

[14] M. Lindroos, M. Apostol, V. Heino, K. Valtonen, A. Laukkanen, K. Holmberg, and V-T. Kuokkala"The deformation, strain hardening, and wear behavior of chromium-alloyed Hadfield steel in abrasive and impact conditions," *Tribol Lett*, vol. 57, pp. 1-11, 2015.

[15] C. Chen, B. Lv, H. Ma, D. Sun, and F. Zhang, "Wear behavior and the corresponding work hardening characteristics of Hadfield steel," *Tribol Int*, vol. 121, pp. 389-399, 2018.

[16] D. K. Subramanyam, G. W. Grube, and H. J. Chapin, "Austenitic manganese steel castings," *ASM Handbook.*, vol. 9, pp. 237-241, 1985.

[17] A. Kamyabi-Gol, and M. Sheikh-Amiri, "Spheroidizing kinetics and optimization of heat treatment parameters in CK60 steel using taguchi robust design," *Journal of Iron and Steel Research International*, vol. 17, no. 4, pp. 45-52, 2010.

[18] G. Tęcza, and S. Sobula, "Effect of heat treatment on change microstructure of cast high-manganese hadfield steel with elevated chromium content," *Archives of Foundry Engineering*, vol. 14, no. 3 spec, pp. 67-70, 2014.

[19] I. El-Mahallawi, R. Abdel-Karim, and A. Naguib, "Evaluation of effect of chromium on wear performance of high manganese steel," *Materials Science and Technology*, vol. 17, no. 11, pp. 1385-1390, 2001.

[20] M. Sabzi, S. M. Far, and S. M. Dezfuli, "Effect of melting temperature on microstructural evolutions, behavior and corrosion morphology of Hadfield austenitic manganese steel in the casting process," *International Journal of Minerals, Metallurgy, and Materials*, vol. 25, pp. 1431-1438, 2018.

[21] J. R. Davis, K. M. Mills, and S. R. Lampman, "Metals handbook. Vol. 1. Properties and selection: irons, steels, and high-performance alloys," *ASM International, Materials Park, Ohio 44073, USA, 1990. 1063*, 1990.

[22] M. K. Banerjee, "2.8 Heat treatment of commercial steels for engineering applications," 2017.

[23] R. F. Mehl, and W. C. Hagel, "The austenite: pearlite reaction," *Progress in Metal Physics*, vol. 6, pp. 74-134, 1956.

[24] W. D. Callister Jr and D. G. Rethwisch, *Callister's materials science and engineering*. John Wiley & Sons, 2020.

[25] ASM Handbook, Vol 1, Properties and selection: irons, steels, and high performance alloys section: Publication information and contributors publication information and contributors authors and reviewers," 2005.

[26] W. S. Rasband, "US National Institutes of Health," *http://imagej. nih. gov/ij/*, 2011.

[27] M. Abbasi, S. Kheirandish, Y. Kharrazi, and J. Hejazi, "The fracture and plastic deformation of aluminum alloyed Hadfield steels," *Materials Science and Engineering: A*, vol. 513, pp. 72-76, 2009.

[28] D. Rittel, and I. Roman, "Tensile fracture of coarse-grained cast austenitic manganese steels," *Metallurgical transactions A*, vol. 19, pp. 2269-2277, 1988.

[29] L. Qian, X. Feng, and F. Zhang, "Deformed microstructure and hardness of Hadfield high manganese steel," *Mater Trans*, vol. 52, no. 8, pp. 1623-1628, 2011.

[30] J. Kowalska, J. Ryś, G. Cios, and W. Bednarczyk, "The effect of reduced temperatures on microstructure development in tensile tested high-manganese steel," *Materials Science and Engineering: A*, vol. 767, p. 138406, 2019.